

# Synthesis and Fluorescence Properties of Thiazole–Boron Complexes Bearing a $\beta$ -Ketoiminate Ligand

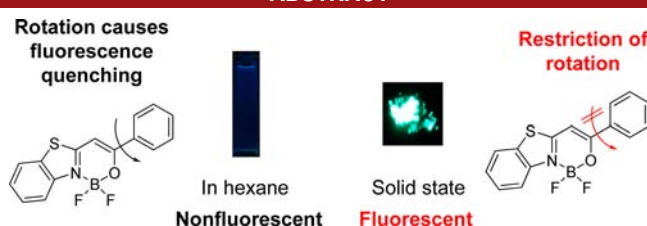
Yasuhiro Kubota,\* Syunki Tanaka, Kazumasa Funabiki, and Masaki Matsui\*

Department of Materials Science and Technology, Faculty of Engineering,  
Gifu University, 1-1 Yanagido, Gifu 501-1193, Japan

kubota@gifu-u.ac.jp; matsui@gifu-u.ac.jp

Received August 5, 2012

## ABSTRACT



Novel fluorescent dyes, thiazole–boron complexes bearing  $\beta$ -ketoiminate ligands, have been synthesized, and their fluorescence properties were investigated. The  $\text{BF}_2$  complexes showed a pronounced aggregation-induced emission enhancement effect because of the restriction of C–Ph intramolecular rotation. The  $\text{BPh}_2$  complexes showed higher fluorescence quantum yields than the corresponding  $\text{BF}_2$  complexes, both in solution and in the solid state.

Most fluorescent dyes that exhibit fluorescence in dilute solutions quench or reduce the fluorescence intensity in the solid state owing to aggregation-caused quenching (ACQ).<sup>1</sup> Recently, Tang et al. have reported unique fluorescent dyes showing aggregation-induced emission enhancement (AIEE) effects which are opposite to the ACQ effect.<sup>2</sup> Owing to their unique fluorescent properties, such AIEE dyes have a wide range of potential applications such as organic electroluminescence devices,<sup>3</sup> fluorescent

sensors,<sup>4</sup> and photodynamic therapy.<sup>5</sup> Thus, AIEE-active molecules such as hydrocarbons<sup>6</sup> and heterocycles<sup>7</sup> have been developed.

Organoboron complexes are one of the most important types of fluorescent dyes. Notably, boron dipyrromethene (BODIPY) dyes<sup>8</sup> have attracted much interest in various fields because of their advantageous properties such as high quantum yield, sharp spectra, and high photostability. However, BODIPY dyes often show a very small Stokes shift and ACQ.<sup>9</sup> The development of novel boron complexes has been aggressively studied.<sup>10</sup> However, little has been published on organoboron complexes showing

(1) (a) Park, S.-Y.; Ebihara, M.; Kubota, Y.; Funabiki, K.; Matsui, M. *Dyes Pigm.* **2009**, *82*, 258. (b) Ooyama, Y.; Okamoto, T.; Yamaguchi, T.; Suzuki, T.; Hayashi, A.; Yoshida, K. *Chem.—Eur. J.* **2006**, *12*, 7827. (c) Shirai, K.; Matsuoka, M.; Fukunishi, K. *Dyes Pigm.* **1999**, *42*, 95.

(2) (a) Hong, Y.; Lam, J. W. Y.; Tang, B. Z. *Chem. Commun.* **2009**, 4332. (b) Hong, Y.; Lam, J. W. Y.; Tang, B. Z. *Chem. Soc. Rev.* **2011**, *40*, 5361.

(3) (a) Li, H.; Chi, Z.; Zhang, X.; Xu, B.; Liu, S.; Zhang, Y.; Xu, J. *Chem. Commun.* **2011**, 11273. (b) Yuan, W. Z.; Chen, S.; Lam, J. W. Y.; Deng, C.; Lu, P.; Sung, H. H.-Y.; Williams, I. D.; Kwok, H. S.; Zhang, Y.; Tang, B. Z. *Chem. Commun.* **2011**, 11216. (c) Zhang, X.; Chi, Z.; Xu, B.; Li, H.; Yang, Z.; Li, X.; Liu, S.; Zhang, Y.; Xu, J. *Dyes Pigm.* **2011**, *89*, 56.

(4) (a) Han, T.; Feng, X.; Tong, B.; Shi, J.; Chen, L.; Zhi, J.; Dong, Y. *Chem. Commun.* **2012**, 416. (b) Sun, F.; Zhang, G.; Zhang, D.; Xue, L.; Jiang, H. *Org. Lett.* **2011**, *13*, 6378. (c) Xu, X.; Huang, J.; Li, J.; Yan, J.; Qin, J.; Li, J. *Chem. Commun.* **2011**, 12385. (d) Shiraiishi, K.; Sanji, T.; Tanaka, M. *Tetrahedron Lett.* **2010**, *51*, 6331. (e) Wang, M.; Zhang, G.; Zhang, D.; Zhu, D.; Tang, B. Z. *J. Mater. Chem.* **2010**, *20*, 1858.

(5) Chang, C.-C.; Hsieh, M.-C.; Lin, J.-C.; Chang, T.-C. *Biomaterials* **2012**, *33*, 897.

(6) (a) Zeng, Q.; Li, Z.; Dong, Y.; Di, C.; Qin, A.; Hong, Y.; Ji, L.; Zhu, Z.; Jim, C. K. W.; Yu, G.; Li, Q.; Li, Z.; Liu, Y.; Qin, J.; Tang, B. Z. *Chem. Commun.* **2007**, 70. (b) Wu, Y.-T.; Kuo, M.-Y.; Chang, Y.-T.; Shin, C.-C.; Wu, T.-C.; Tai, C.-C.; Cheng, T.-H.; Liu, W.-S. *Angew. Chem., Int. Ed.* **2008**, *47*, 9891. (c) Kokado, K.; Chujo, Y. *J. Org. Chem.* **2011**, *76*, 316. (d) Feng, J.; Chen, X.; Han, Q.; Wang, H.; Lu, P.; Wang, Y. *J. Lumin.* **2011**, *131*, 2775. (e) Hirose, T.; Higashiguchi, K.; Matsuda, K. *Chem.—Asian J.* **2011**, *6*, 1057. (f) Wang, W.; Lin, T.; Wang, M.; Liu, T.-X.; Ren, L.; Chen, D.; Huang, S. *J. Phys. Chem. B* **2010**, *114*, 5983. (g) Tong, H.; Dong, Y.; Haeussler, M.; Lam, J. W. Y.; Sung, H. H.-Y.; Williams, I. D.; Sun, J.; Tang, B. Z. *Chem. Commun.* **2006**, 1133. (h) Shimizu, M.; Tatsumi, H.; Mochida, K.; Shimono, K.; Hiyama, T. *Chem.—Asian J.* **2009**, *4*, 1289. (i) Li, H.; Chi, Z.; Xu, B.; Zhang, X.; Li, X.; Liu, S.; Zhang, Y.; Xu, J. *J. Mater. Chem.* **2011**, *21*, 3760. (j) Liang, Z.-Q.; Li, Y.-X.; Yang, J.-X.; Ren, Y.; Tao, X.-T. *Tetrahedron Lett.* **2011**, *52*, 1329. (k) Kim, S.; Zheng, Q.; He, G. S.; Bharali, D. J.; Pudavar, H. E.; Baev, A.; Prasad, P. N. *Adv. Funct. Mater.* **2006**, *16*, 2317.

AIEE effects. To the best of our knowledge, only two types of AIEE active boron complexes, BODIPY<sup>11</sup> and BF<sub>2</sub>–hydrazone (BODIHY),<sup>12</sup> have been reported thus far. Recently, we reported that pyrazine–boron complexes having a  $\beta$ -ketoiminato ligand show a large Stokes shift and solid-state fluorescence.<sup>13</sup> In this paper, we report the synthesis and fluorescence properties of thiazole–boron complexes bearing  $\beta$ -ketoiminato ligands, which show the AIEE effect.

The reaction of 2-methylbenzothiazole with methyl benzoate gave benzothiazole-based  $\beta$ -ketoiminato ligand **1** (Scheme S1). In solution, ligand **1** exists in two tautomeric forms, iminoketone **1a** and iminoenol **1b**, through keto–enol tautomerization. The structure of **1a** was confirmed by the methylene signal at  $\delta$  4.84 (s, 2H) in its <sup>1</sup>H NMR spectrum. Tautomer **1b** was also confirmed by the <sup>1</sup>H NMR signals at  $\delta$  6.38 (s, 1H, C=CH) and 13.9 (brs, 1H, OH). The ratio of **1a** and **1b** was 1:1.5 in CDCl<sub>3</sub>. The tautomeric mixture **1** was then allowed to react with the boron trifluoride–diethyl ether complex in the presence of triethylamine in dichloromethane to afford the

corresponding BF<sub>2</sub> complex, **2** (Scheme S2). The reaction of **1** with triphenylborane also gave corresponding BPh<sub>2</sub> complex **3**. The structures of **2** and **3** were confirmed by X-ray crystallography (Figures S1 and S2).

The absorption and fluorescence spectra of **1–3** in hexane are shown in Figure 1. The BF<sub>2</sub> complex **2** showed a sharp absorption peak at 380 nm along with a vibrational peak. In contrast, BPh<sub>2</sub> complex **3** exhibited a structureless absorption spectrum. The maximum absorption wavelength ( $\lambda_{\text{max}}$ ) of **3** (402 nm) was more bathochromic than that of **2** (380 nm), and the molar absorption coefficient ( $\epsilon$ ) of **3** (25,800) was lower than that of **2** (43,700) (Table 1). This red shift of  $\lambda_{\text{max}}$  and decrease in  $\epsilon$  of **3** may be due to the molecular bending of the BPh<sub>2</sub> complex caused by the introduction of bulky phenyl groups at the boron atom.<sup>13,14</sup>

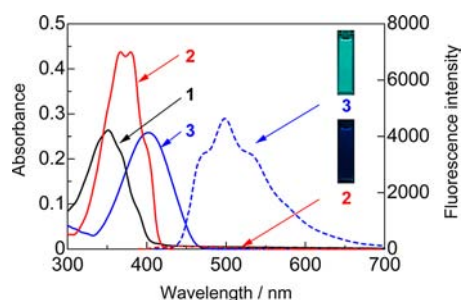


**Figure 1.** UV–vis absorption and fluorescence spectra of **1–3** in hexane.

(7) (a) Luo, J.; Xie, Z.; Lam, J. W. Y.; Cheng, L.; Chen, H.; Qiu, C.; Kwok, H. S.; Zhan, X.; Liu, Y.; Zhu, D.; Tang, B. Z. *Chem. Commun.* **2001**, 1740. (b) Wang, B.; Wang, Y.; Hua, J.; Jiang, Y.; Huang, J.; Qian, S.; Tian, H. *Chem.—Eur. J.* **2011**, *17*, 2647. (c) Kamino, S.; Horio, Y.; Komeda, S.; Minoura, K.; Ichikawa, H.; Horigome, J.; Tatsumi, A.; Kaji, S.; Yamaguchi, T.; Usami, Y.; Hirota, S.; Enomoto, S.; Fujita, Y. *Chem. Commun.* **2010**, 9013. (d) Shiraishi, K.; Kashiwabara, T.; Sanji, T.; Tanaka, M. *New J. Chem.* **2009**, *33*, 1680. (e) Xu, B.; He, J.; Dong, Y.; Chen, F.; Yu, W.; Tian, W. *Chem. Commun.* **2011**, 6602. (f) Matsui, M.; Noguchi, K.; Kubota, Y.; Funabiki, K. *Tetrahedron* **2010**, *66*, 9396. (g) Li, H.; Chi, Z.; Xu, B.; Zhang, X.; Yang, Z.; Li, X.; Liu, S.; Zhang, Y.; Xu, J. *J. Mater. Chem.* **2010**, *20*, 6103. (h) Li, H.; Zhang, X.; Chi, Z.; Xu, B.; Zhou, W.; Liu, S.; Zhang, Y.; Xu, J. *Org. Lett.* **2011**, *13*, 556.

(8) (a) Loudet, A.; Burgess, K. *Chem. Rev.* **2007**, *107*, 4891. (b) Ulrich, G.; Ziesse, R.; Harriman, A. *Angew. Chem., Int. Ed.* **2008**, *47*, 1184. (c) Benstead, M.; Mehl, G. H.; Boyle, R. W. *Tetrahedron* **2011**, *67*, 3573. (d) Hong, H.; Wang, Z.; Yang, J.; Zheng, Q.; Zong, S.; Sheng, Y.; Zhu, D.; Tang, C.; Cui, Y. *Analyst* **2012**, *137*, 4140.

(9) (a) Zhang, D.; Wen, Y.; Xiao, Y.; Yu, G.; Liu, Y.; Qian, X. *Chem. Commun.* **2008**, 4777. (b) Hepp, A.; Ulrich, G.; Schmechel, R.; Von Seggern, H.; Ziesse, R. *Synth. Met.* **2004**, *146*, 11. (c) Kubota, Y.; Uehara, J.; Funabiki, K.; Matsui, M. *Tetrahedron. Lett.* **2010**, *51*, 6195.

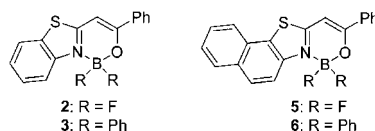
(10) (a) Araneda, J. F.; Piers, W. E.; Heyne, B.; Parvez, M.; McDonald, R. *Angew. Chem., Int. Ed.* **2011**, *50*, 12214. (b) Ito, F.; Nagai, T.; Ono, Y.; Yamaguchi, K.; Furuta, H.; Nagamura, T. *Chem. Phys. Lett.* **2007**, *435*, 283. (c) Kubota, Y.; Tsuzuki, T.; Funabiki, K.; Ebihara, M.; Matsui, M. *Org. Lett.* **2010**, *12*, 4010. (d) Bañuelos, J.; López Arbeloa, F.; Martínez, V.; Liras, M.; Costela, A.; García Moreno, I.; López Arbeloa, I. *Phys. Chem. Chem. Phys.* **2011**, *13*, 3437. (e) Zhou, Y.; Xiao, Y.; Li, D.; Fu, M.; Qian, X. *J. Org. Chem.* **2008**, *73*, 1571. (f) Ito, F.; Nagai, T.; Ono, Y.; Yamaguchi, K.; Furuta, H.; Nagamura, T. *Chem. Phys. Lett.* **2007**, *435*, 283. (g) Hachiya, S.; Inagaki, T.; Hashizume, D.; Maki, S.; Niwa, H.; Hirano, T. *Tetrahedron. Lett.* **2010**, *51*, 1613. (h) Fischer, G. M.; Ehlers, A. P.; Zumbusch, A.; Daltrozzo, E. *Angew. Chem., Int. Ed.* **2007**, *46*, 3750. (i) Ono, K.; Hashizume, J.; Yamaguchi, H.; Tomura, M.; Nishida, J.; Yamashita, Y. *Org. Lett.* **2009**, *11*, 4326. (j) Feng, J.; Liang, B.; Wang, D.; Xue, L.; Li, X. *Org. Lett.* **2008**, *10*, 4437. (k) Zhou, Y.; Xiao, Y.; Chi, S.; Qian, X. *Org. Lett.* **2008**, *10*, 633. (l) Nagai, A.; Kokado, K.; Nagata, Y.; Arita, M.; Chujo, Y. *J. Org. Chem.* **2008**, *73*, 8605. (m) Yan, W.; Wan, X.; Chen, Y. *J. Mol. Struct.* **2010**, *968*, 85. (n) Xia, M.; Wu, B.; Xiang, G. *J. Fluor. Chem.* **2008**, *129*, 402. (o) Kobayashi, N.; Takeuchi, Y.; Matsuda, A. *Angew. Chem., Int. Ed.* **2007**, *46*, 758. (p) Wu, L.; Burgess, K. *J. Am. Chem. Soc.* **2008**, *130*, 4089. (q) Mao, M.; Xiao, S.; Yi, T.; Zou, K. *J. Fluor. Chem.* **2011**, *132*, 612.

(11) Hu, R.; Lager, E.; Aguilar-Aguilar, A.; Liu, J.; Lam, J. W. Y.; Sung, H. H. Y.; Williams, I. D.; Zhong, Y.; Wong, K. S.; Peña-Cabrera, E.; Tang, B. Z. *J. Phys. Chem. C* **2009**, *113*, 15845.

(12) Yang, Y.; Su, X.; Carroll, C. N.; Aprahamian, I. *Chem. Sci.* **2012**, *3*, 610.

(13) Kubota, Y.; Hara, H.; Tanaka, S.; Funabiki, K.; Matsui, M. *Org. Lett.* **2011**, *13*, 6544.

**Table 1.** UV–vis Absorption and Fluorescence Properties



compd	in hexane <sup>a</sup>						solid state	
	$\lambda_{\text{max}}$ ( $\epsilon$ ) (nm)	$F_{\text{max}}^b$ (nm)	$\phi_f^{b,c}$	$\tau_f^d$ (ns)	$k_f^e$ ( $10^9 \text{ s}^{-1}$ )	$k_{nr}^f$ ( $10^9 \text{ s}^{-1}$ )	$F_{\text{max}}^g$ (nm)	$\phi_f^{c,g}$
<b>2</b>	380 (43,700)	440	<0.01	— <sup>h</sup>	—	—	495	0.26
<b>3</b>	402 (25,800)	499	0.41	2.9	0.14	0.20	503	0.60
<b>5</b>	396 (39,900)	459	0.04	0.13	0.31	7.38	508	0.23
<b>6</b>	406 (18,600)	510	0.49	3.0	0.16	0.17	527	0.50

<sup>a</sup> Measured at a concentration of  $1.0 \times 10^{-5} \text{ mol dm}^{-3}$ . <sup>b</sup> The excitation wavelengths ( $\lambda_{\text{ex}}$ ) were as follows: **2** (380 nm), **3** (400 nm), **5** (394 nm), and **6** (412 nm). <sup>c</sup> Measured using a Quantaaurus-QY. <sup>d</sup> Measured using a Quantaaurus- $\tau$ . <sup>e</sup> Radiative rate constant ( $k_f = \Phi_f/\tau_f$ ). <sup>f</sup> Nonradiative rate constant ( $k_{nr} = (1 - \Phi_f)/\tau_f$ ). <sup>g</sup> The  $\lambda_{\text{ex}}$  were as follows: **2** (429 nm), **3** (440 nm), **5** (425 nm), and **6** (492 nm). <sup>h</sup> Too short to be measured by the Quantaaurus- $\tau$  ( $\tau_f < 0.1 \text{ ns}$ ).

(14) (a) Brooker, L. G. S.; White, F. L.; Sprague, R. H.; Dent, S. G.; Van Zandt, G. *Chem. Rev.* **1947**, *41*, 325. (b) Longuet-Higgins, H. C. *J. Chem. Phys.* **1950**, *18*, 265.

The solvent effect on the absorption and fluorescence properties of **2** and **3** was examined (Figures S3–S6; Tables 2 and S1). The  $\lambda_{\text{max}}$  and  $\epsilon$  values of **2** and **3** were hardly affected by solvent polarity, suggesting that the dipole moments of the molecules in the ground and excited states were almost the same.<sup>3a</sup> Contrary to our expectation, BF<sub>2</sub> complex **2** hardly exhibited fluorescence in solution. The absolute fluorescence quantum yields ( $\Phi_f$ ) of **2** were only as high as 0.01 in low-viscosity solvents (Table 2). On the other hand, BPh<sub>2</sub> complex **3** showed relatively strong fluorescence along with two vibrational peaks in solution (Table S1). The maximum fluorescence wavelengths ( $F_{\text{max}}$ ) showed almost no variation with changing solvent polarity (497–502 nm), and the values of  $\Phi_f$  in polar solvents (MeOH, 0.17; MeCN, 0.25) were lower compared with those in other solvents (hexane, 0.41; toluene, 0.46; CHCl<sub>3</sub>, 0.46; THF, 0.46; CH<sub>2</sub>Cl<sub>2</sub>, 0.42). Complex **3** exhibited a relatively large Stokes shift (4770–5070 cm<sup>-1</sup>) than fluorescent boron complexes such as BODIPY dyes<sup>12</sup> (400–600 cm<sup>-1</sup>) and pyridomethene–BF<sub>2</sub> complexes<sup>12</sup> (250–400 cm<sup>-1</sup>).

**Table 2.** UV–vis Absorption and Fluorescence Properties of **2** in Various Solvents<sup>a</sup>

solvent	dielectric constant	viscosity (cP at 20°C)	$\lambda_{\text{max}}$ ( $\epsilon$ ) (nm)	$F_{\text{max}}$ <sup>b</sup> (nm)	$\phi_f$ <sup>c</sup>	$\tau_f$ <sup>d</sup> (ns)	$k_f$ <sup>e</sup> (10 <sup>9</sup> s <sup>-1</sup> )	$k_{\text{nr}}$ <sup>f</sup> (10 <sup>9</sup> s <sup>-1</sup> )
Hexane	1.9	0.31	380 (43,700)	440	<0.01	— <sup>g</sup>	—	—
Toluene	2.4	0.59	384 (42,300)	448	0.01	— <sup>g</sup>	—	—
CHCl <sub>3</sub>	4.8	0.57	382 (45,300)	444	0.01	— <sup>g</sup>	—	—
THF	7.6	0.55	382 (45,300)	443	0.01	— <sup>g</sup>	—	—
CH <sub>2</sub> Cl <sub>2</sub>	8.9	0.44	382 (47,000)	444	0.01	— <sup>g</sup>	—	—
MeOH	33	0.55	379 (38,800)	440	<0.01	— <sup>g</sup>	—	—
MeCN	38	0.38	378 (44,100)	441	<0.01	— <sup>g</sup>	—	—
Ethylene glycol	39	23.5	383 (41,600)	444	0.05	0.18	0.28	5.28
Glycerol	47	1412	389 (36,000)	449	0.12	0.64	0.19	1.38

<sup>a</sup> Measured at a concentration of  $1.0 \times 10^{-5}$  mol dm<sup>-3</sup>. <sup>b</sup> The excitation wavelengths ( $\lambda_{\text{ex}}$ ) were as follows: hexane (380 nm), toluene (382 nm), chloroform (381 nm), THF (381 nm), dichloromethane (382 nm), methanol (379 nm), acetonitrile (378 nm), ethylene glycol (382 nm), and glycerol (389 nm). <sup>c</sup> Measured using a Quantaaurus-QY. <sup>d</sup> Measured using a Quantaaurus- $\tau$ . <sup>e</sup> Radiative rate constant ( $k_f = \Phi_f/\tau_f$ ). <sup>f</sup> Nonradiative rate constant ( $k_{\text{nr}} = (1 - \Phi_f)/\tau_f$ ). <sup>g</sup> Too short to be measured by the Quantaaurus- $\tau$  (<0.1 ns).

A similar reaction of 2-methylnaphtho[2,1-*d*]thiazole with acetophenone gave naphthothiazole-based  $\beta$ -ketoiminate ligand **4** (Scheme S3). Corresponding BF<sub>2</sub> complex **5** and BPh<sub>2</sub> complex **6** were obtained by the reaction of **4** with the trifluoride–diethyl ether complex and triphenylborane, respectively (Scheme S4). The absorption and fluorescence spectra in hexane are shown in Figures S7 and S8. The  $\lambda_{\text{max}}$  and  $F_{\text{max}}$  values of naphthothiazole derivatives **5** ( $\lambda_{\text{max}} = 396$  nm,  $F_{\text{max}} = 459$  nm) and **6** ( $\lambda_{\text{max}} = 406$  nm,  $F_{\text{max}} = 510$  nm) were slightly red-shifted compared with those of the corresponding benzothiazole derivatives **2** ( $\lambda_{\text{max}} = 380$  nm,  $F_{\text{max}} = 440$  nm) and **3** ( $\lambda_{\text{max}} = 402$  nm,  $F_{\text{max}} = 499$  nm), owing to the extension of  $\pi$ -conjugation (Table 1). To understand the absorption

properties, density functional theory (DFT) calculations were performed with the Gaussian 09 package.<sup>15</sup> The geometries of **2**, **3**, **5**, and **6** were optimized at the B3LYP/6-31G(d,p) level. Time-dependent DFT (TDDFT) calculations were also performed at the B3LYP/6-311++G(d,p) level. The calculated  $\lambda_{\text{max}}$ , the main orbital transition, and oscillator strength  $f$  are shown in Table S2. These calculated values of  $\lambda_{\text{max}}$  and  $f$  are in good agreement with the experimental values. For all complexes, the first absorptions are mainly attributed to the transitions from HOMO to LUMO. For each complex, the HOMO and LUMO orbitals are delocalized over the entire molecule (Figure S9).

To determine whether thiazole–boron complexes have AIEE character, the fluorescence properties of **2** were investigated in THF–water mixtures of various ratios, since **2** is soluble in THF but not in water. The fluorescence properties were almost the same until the addition of 70% water by volume, because **2** was soluble in the THF–water mixtures with a lower water content. However, upon addition of 80% water in THF, the fluorescence color and  $F_{\text{max}}$  changed dramatically from blue to yellow-green and from 445 to 495 nm, respectively (Figure S10). The fluorescence intensity also increased with the increasing water content of the solvent (Figure S11). Notably, the intensity was significantly enhanced when the water fraction exceeded 80%. These changes result from the formation of aggregates in the THF–water mixtures. When the water content was increased to 80%, the absorption spectra exhibited leveled-off tails extending into the long-wavelength region (Figure S12). This may be due to Mie light scattering caused by nanoparticles.<sup>6j,7c</sup> The Tyndall phenomenon was observed when the 80% THF/water solution was irradiated by laser light (Figure S13). This also suggests the formation of nanoparticles. Similar results were observed for naphthothiazole derivative **5** (Figures S14 and 15). Therefore, BF<sub>2</sub> complexes are considered to have AIEE character.

To determine the reason for the AIEE effect in the complexes, time-resolved fluorescence spectroscopy was performed. The fluorescence decays were fitted to a mono-exponential function. The fluorescence lifetimes ( $\tau_f$ ) of **3**, **5**, and **6** in hexane were measured to be 2.9, 0.13, and 3.0 ns, respectively; however, the lifetime of **2** was too short to measure (<0.1 ns). The radiative ( $k_f = \Phi_f/\tau_f$ ) and non-radiative ( $k_{\text{nr}} = (1 - \Phi_f)/\tau_f$ ) rate constants were also

(15) Frisch, M. J.; Trucks, G. W.; Schlegel, H. B.; Scuseria, G. E.; Robb, M. A.; Cheeseman, J. R.; Montgomery, J. A., Jr.; Vreven, T.; Kudin, K. N.; Burant, J. C.; Millam, J. M.; Iyengar, S. S.; Tomasi, J.; Barone, V.; Mennucci, B.; Cossi, M.; Scalmani, G.; Rega, N.; Petersson, G. A.; Nakatsuji, H.; Hada, M.; Ehara, M.; Toyota, K.; Fukuda, R.; Hasegawa, J.; Ishida, M.; Nakajima, T.; Honda, Y.; Kitao, O.; Nakai, H.; Klene, M.; Li, X.; Knox, J. E.; Hratchian, H. P.; Cross, J. B.; Adamo, C.; Jaramillo, J.; Gomperts, R.; Stratmann, R. E.; Yazyev, O.; Austin, A. J.; Cammi, R.; Pomelli, C.; Ochterski, J. W.; Ayala, P. Y.; Morokuma, K.; Voth, G. A.; Salvador, P.; Dannenberg, J. J.; Zakrzewski, V. G.; Dapprich, S.; Daniels, A. D.; Strain, M. C.; Farkas, O.; Malick, D. K.; Rabuck, A. D.; Raghavachari, K.; Foresman, J. B.; Ortiz, J. V.; Cui, Q.; Baboul, A. G.; Clifford, S.; Cioslowski, J.; Stefanov, B. B.; Liu, G.; Liashenko, A.; Piskorz, P.; Komaromi, I.; Martin, R. L.; Fox, D. J.; Keith, T.; Al-Laham, M. A.; Peng, C. Y.; Nanayakkara, A.; Challacombe, M.; Gill, P. M. W.; Johnson, B.; Chen, W.; Wong, M. W.; Gonzalez, C.; Pople, J. A. *Gaussian 09, revision A. 02*; Gaussian, Inc.: Wallingford, CT, 2009.

calculated (Table 1). Although there was little difference between the  $k_f$  values of BF<sub>2</sub> complex **5** ( $0.31 \times 10^9 \text{ s}^{-1}$ ) and the BPh<sub>2</sub> complexes (**3**,  $0.14 \times 10^9$ ; **6**,  $0.16 \times 10^9 \text{ s}^{-1}$ ), the  $k_{nr}$  of **5** ( $7.4 \times 10^9 \text{ s}^{-1}$ ) was obviously larger than those of **3** ( $0.20 \times 10^9 \text{ s}^{-1}$ ) and **6** ( $0.17 \times 10^9 \text{ s}^{-1}$ ). This suggests that the lower fluorescence quantum yields of the BF<sub>2</sub> complexes are attributed to an increase in nonradiative processes. To obtain further insight, we investigated the effect of solvent viscosity and temperature on fluorescence. Regardless of the solvent polarity, BF<sub>2</sub> complex **2** hardly showed fluorescence ( $\Phi_f \leq 0.01$ ) in low-viscosity solvents (0.31–0.59 cP) (Figure S4 and Table 2). On the other hand, **2** exhibited fluorescence in ethylene glycol ( $\Phi_f = 0.05$ , 23.5 cP) and glycerol ( $\Phi_f = 0.12$ , 1412 cP). This suggests that the viscous medium inhibits intramolecular rotation, thereby suppressing the nonradiative process which leads to increased  $\Phi_f$ .<sup>16</sup> The fluorescence intensity of **2** in hexane increased gradually as the temperature decreased (Figure S16). This also suggests that the restriction of intramolecular rotation (RIR) associated with decreasing temperature leads to enhanced fluorescence. Therefore, the main reason for AIEE of **2** is considered to be the RIR associated with the phenyl group.

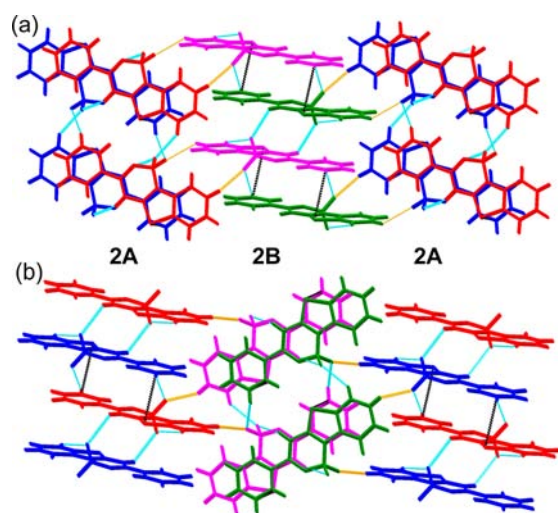


**Figure 2.** (a) Top view of the crystal structure of **2** ( $Z = 4$ ,  $Z' = 2$ ). (b) Side view of the crystal structure of **2**. Red and blue molecules show **2A**. Pink and green molecules show **2B**. The black, light blue, and orange dotted lines show intermolecular C $\cdots$ S, CH/F interactions of **2A** or **2B**, and CH/F interactions between **2A** and **2B**, respectively.

All thiazole–boron complexes, **2**, **3**, **5**, and **6**, showed fluorescence in the solid state (Figure S17). The solid-state absorption spectra of **2**, **3**, **5**, and **6** are shown in Figure S18. The absorption spectra in the solid state were broader and red-shifted compared to those in the solution. As a result, the  $F_{\text{max}}$  values in the solid state (495–527 nm) were more

(16) (a) Bloor, D.; Kagawa, Y.; Szablewski, M.; Ravi, M.; Clark, S. J.; Cross, G. H.; Palsson, L.-O.; Beeby, A.; Parmerc, C.; Rumbles, G. *J. Mater. Chem.* **2001**, *11*, 3053. (b) Barbara, P. F.; Rand, S. D.; Rentzepis, P. M. *J. Am. Chem. Soc.* **1981**, *103*, 2156.

bathochromic than those in hexane (440–510 nm). Similar to the results obtained in solution, BPh<sub>2</sub> complexes **3** and **6** showed higher  $\Phi_f$  values (0.60 and 0.50, respectively) than the corresponding BF<sub>2</sub> complexes **2** (0.26) and **5** (0.23) in the solid state (Table 1). To consider the difference, we investigated the crystal packing. Two independent crystallographic conformers, **2A** and **2B**, were observed in the crystal of **2** ( $Z' = 2$ ) (Figure S1). In the crystal packing of **2**, **2A** and **2B** formed independent stacking columns (Figures 2 and S19). Each stacking column formed consecutive intermolecular interactions by C $\cdots$ S (**2A**, 3.64 Å; **2B**, 3.68 Å) and CH/F interactions (**2A**, 2.41–2.66 Å; **2B**, 2.47–2.66 Å). Furthermore, CH/F interactions were also observed between **2A** and **2B** (2.41–2.56 Å). As a result, BF<sub>2</sub> complex **2** formed consecutive intermolecular interactions throughout the molecule. In the case of BPh<sub>2</sub> complex **3**, similar to BF<sub>2</sub> complex **2**, stacking columns having consecutive intermolecular interactions were formed through C $\cdots$ S (3.70 Å) and CH/ $\pi$  interactions (2.85–2.89 Å) (Figure S20). Since the CH/ $\pi$  interaction is weaker than CH/F interactions, the intramolecular interactions of stacking columns of **3** are weaker than those of **2**. Additionally, unlike BF<sub>2</sub> complex **2**, interactions between stacking columns were not observed in **3**. Because CH/F interactions were inhibited, BPh<sub>2</sub> complex **3** exhibited a higher  $\Phi_f$  than did BF<sub>2</sub> complex **2** in the solid state.

In summary, thiazole–boron complexes bearing  $\beta$ -ketoiminate ligands have been synthesized. Although the BF<sub>2</sub> complexes hardly showed fluorescence in hexane ( $F_{\text{max}}$ : 440–459 nm,  $\Phi_f \leq 0.04$ ), the BPh<sub>2</sub> complexes exhibited relatively strong fluorescence ( $F_{\text{max}}$ , 499–510 nm;  $\Phi_f$ , 0.41–0.49). Time-resolved fluorescence spectroscopy revealed that the lower values of  $\Phi_f$  for the BF<sub>2</sub> complexes are attributed to the promotion of nonradiative processes. The BPh<sub>2</sub> complexes also showed higher  $\Phi_f$  values in the solid state ( $F_{\text{max}}$ , 503–527 nm;  $\Phi_f$ , 0.50–0.60) compared with those of the BF<sub>2</sub> complexes ( $F_{\text{max}}$ , 495–508 nm;  $\Phi_f$ , 0.23–0.26). X-ray crystallographic analysis suggested that the lower  $\Phi_f$  of the BF<sub>2</sub> complexes is due to the formation of consecutive intermolecular CH/F interactions. These complexes exhibited higher  $\Phi_f$  values in the solid state than in solution; in other words, thiazole–boron complexes have AIEE character. The  $\Phi_f$  in solution became higher and the nonradiative process was suppressed as the solvent viscosity increased, indicating that the main reason for AIEE in the complexes is the restriction of intramolecular C–Ph rotation. Since intramolecular rotations are inhibited in the solid state, the thiazole–boron complexes are considered to show higher  $\Phi_f$  values in the solid state than in solution.

**Acknowledgment.** This work was supported by Grant-in-Aid for Young Scientists (B) (23750228).

**Supporting Information Available.** Details of experimental procedures and copies of <sup>1</sup>H, <sup>13</sup>C NMR, and 2D spectra for new compounds. This material is available free of charge via the Internet at <http://pubs.acs.org>.

The authors declare no competing financial interest.